

Conjugate priors for count and rounded data regression

Daniel R. Kowal*

Abstract

Discrete data are abundant and often arise as counts or rounded data. However, even for linear regression models, conjugate priors and closed-form posteriors are typically unavailable, thereby necessitating approximations or Markov chain Monte Carlo for posterior inference. For a broad class of count and rounded data regression models, we introduce conjugate priors that enable closed-form posterior inference. Key posterior and predictive functionals are computable analytically or via direct Monte Carlo simulation. Crucially, the predictive distributions are discrete to match the support of the data and can be evaluated or simulated jointly across multiple covariate values. These tools are broadly useful for linear regression, nonlinear models via basis expansions, and model and variable selection. Multiple simulation studies demonstrate significant advantages in computing, predictive modeling, and selection relative to existing alternatives.

KEYWORDS: Bayesian statistics; discrete data; generalized linear models; integer data; prediction.

1 Introduction

Discrete data commonly arise either as natural counts or via data coarsening such as rounding. Bayesian regression models must account for this discreteness in order to provide a coherent data-generating process. However, discrete data often present challenging distributional features, including zero-inflation, over/under-dispersion, boundedness or censoring, and heaping. Customized Bayesian models that target these features are usually too complex for analytical posterior and predictive analysis and can incur significant computational burdens from the requisite approximation algorithms, such as Markov chain Monte Carlo. The contribution of this paper is to provide conjugate priors, closed-form posteriors, and efficient Monte Carlo posterior and predictive simulation algorithms for a broad class of discrete data regression models.

The impact of data coarsening is often nonignorable, both for coherency of the data-generating process and for correct and efficient inference. Dempster and Rubin (1983) emphasized the surprisingly large impact of rounded data adjustments in least squares regression, which notably do not decay with the sample size. More broadly, Heitjan (1989) reviewed inference and asymptotics for grouped data, where continuous data are observable only up to some coarsening such as an interval. Heitjan and Rubin (1991) studied multiple sources of data coarsening, including rounding, heaping, and, censoring, as well as random coarsening operators.

*Dobelman Family Assistant Professor, Department of Statistics, Rice University (daniel.kowal@rice.edu)

The perspective on discrete data offered by grouping or rounding has also been popularized as a modeling strategy for count and binary data. Canale and Dunson (2011) introduced rounded Gaussian mixture models for count-valued Bayesian nonparametrics, while Canale and Dunson (2013) similarly applied rounded Gaussian processes for count regression modeling. Kowal and Canale (2020) developed extensions that incorporated both rounding and transformation operators to adapt linear, additive, and BART regression models for count and rounded data. Although these works demonstrate the utility of discretized continuous data models for count data, none of these methods provides analytic posterior or predictive distributions, and instead use Markov chain Monte Carlo for inference. Among related non-Bayesian approaches, Siegfried and Hothorn (2020) and Kowal and Wu (2021) developed count data regression with an emphasis on learning a transformation for more adaptive discrete distributional modeling. A similar strategy was deployed by Jia et al. (2021) for count time series analysis.

Conjugate priors for discrete data regression have received renewed attention, including for binary (Durante, 2019) and multinomial (Fasano and Durante, 2020) data. Indeed, the closed-form posteriors for probit linear regression derived by Durante (2019) are a special case of our results. However, there are additional challenges in our setting. First, our results generalize from binary data $y \in \{0, 1\}$ to discrete data $y \in \mathbb{Z}$, including count data, rounded data, and bounded or censored (discrete) data. These generalizations require a different class of distributions for conjugate modeling, and therefore distinct descriptions and computations of the relevant posterior and predictive quantities. Second, our framework incorporates a transformation, which is irrelevant for binary data but widely-used in count data models. For instance, count data are often modeled (incoherently) using continuous regression models after log or square-root transformations, while copula models incorporate transformations via the marginal distributions (Pitt et al., 2006). Third, we prioritize closed-form predictive distributions that are discrete to match the support of the data and joint across multiple covariate values. Naturally, a predictive distribution supported on (a subset of) \mathbb{Z} is a substantial generalization of a binary predictive distribution, which is completely characterized by the success probability $\text{pr}(\tilde{y} = 1 \mid y)$. Our results admit direct predictive probability evaluations and Monte Carlo predictive sampling for discrete data $y \in \mathbb{Z}$, including for sparse regression, nonlinear models, and model-averaged scenarios.

Bayesian regression models for count data commonly build upon the Poisson distribution. Except in special cases, the posterior and predictive distributions do not have known closed forms and therefore require approximations such as Markov chain Monte Carlo. Further, the Poisson distribution is often inadequate for modeling, especially in the case of over/under-dispersion, zero-inflation, or heaping. Generalizations such as the Conway-Maxwell-Poisson distribution (Sellers and Shmueli, 2010) or the discrete Weibull distribution (Peluso et al., 2019) provide more flexible count distribution models, yet are burdened by more intensive computations. Polson et al. (2013) introduced a data augmentation strategy for Gibbs sampling with Negative Binomial likelihoods, while Bradley et al. (2018) proposed log-gamma distributions that are conditionally conjugate to the Poisson distribution. These approaches employ Markov chain Monte Carlo for all posterior and predictive inference and typically require further modifications to account for zero-inflation, bounded or censored data, and heaping.

2 Conjugate priors for count and rounded data

2.1 Transformation and rounding models

For paired data $\{(x_i, y_i)\}_{i=1}^n$ with covariates $x_i \in \mathbb{R}^p$ and integer-valued responses $y_i \in \mathbb{Z}$, consider the following class of models:

$$y_i = h \circ g^{-1}(z_i) \quad (1)$$

$$z_i \sim \Pi_\theta(\cdot \mid x_i) \quad (2)$$

where $h : \mathbb{R} \rightarrow \mathbb{Z}$ is a *rounding operator*, $g : \mathbb{R} \rightarrow \mathbb{R}$ is a (monotone increasing) *transformation*, and $\Pi_\theta(\cdot \mid x_i)$ is a covariate-dependent *continuous distribution* parametrized by θ . Informally, (1)–(2) is designed to adapt a continuous data model Π_θ for coherent modeling of discrete data $\{y_i\}_{i=1}^n$. We focus primarily on the Gaussian linear model for the latent continuous data z_i ,

$$z_i = x_i' \theta + \epsilon_i, \quad \epsilon_i \sim N(0, \sigma^2) \quad (3)$$

independently for $i = 1, \dots, n$, with modifications available for heteroskedastic or dependent errors and nonlinear versions (see Section 2.5).

It is useful to decouple the rounding operator h , which defines the support of y , and the transformation g , which is a smooth monotone function. First, consider the rounding operator h , which is defined via a partition $\{\mathcal{A}_j\}$ of \mathbb{Z} such that $y_i = j$ whenever $z_i \in g(\mathcal{A}_j)$.

Example 1. Suppose that we observe rounded data instead of continuous data. Let the rounded digit be the first decimal place, which can be satisfied by pre-multiplying the data by the appropriate power of 10 such that $y \in \mathbb{Z}$. When $g(t) = t$ is the identity, z_i represents the unobserved continuous data version of y_i . In this case, $y_i = j$ whenever $z_i \in \mathcal{A}_j = [j - 0.5, j + 0.5)$, so $h(t) = \lfloor t + 0.5 \rfloor$ and $\lfloor \cdot \rfloor$ is the floor function.

Example 2. Suppose that $y \in \{0, \dots, y_{max}\}$ is count-valued and bounded by some known y_{max} . The rounding operator defined by $h(t) = 0$ for $t < 1$, $h(t) = \lfloor t \rfloor$ for $t \in [1, y_{max}]$, and $h(t) = y_{max}$ for $t > y_{max}$ ensures the correct support for the data-generating process. Equivalently, the partition is $\mathcal{A}_0 = (-\infty, 1)$, $\mathcal{A}_j = [j, j + 1)$ for $j = 1, \dots, y_{max} - 1$, and $\mathcal{A}_{y_{max}} = [y_{max}, \infty)$. In addition, (1)–(2) coupled with this choice of h produces a valid likelihood for censored data (Kowal and Canale, 2020). The case of unbounded counts simply requires $y_{max} = \infty$. When $y_{max} = 1$, our results reproduce Durante (2019) for probit regression.

Next, consider the monotone increasing transformation g .

Example 3. The (signed) Box-Cox family (Box and Cox, 1964) provides a parametric option, $g(t; \lambda) = \{\text{sgn}(t)|t|^\lambda\}/\lambda$, for $\lambda > 0$ with $g(t; \lambda = 0) = \log(t)$ for $t > 0$. In addition to the log transformation, this family includes the (shifted and scaled) identity ($\lambda = 1$) and square-root ($\lambda = 1/2$) transformations. These transformations are common for (incoherent) application of continuous models (2) to count data without the rounding operator h ; for example, the square-root transformation is the variance-stabilizing transformation of the Poisson distribution. Kowal and Canale (2020) used this family for Bayesian modeling of (1)–(2).

Example 4. Using copula-style models, an alternative strategy is to link the transformation to the cumulative distribution function of y (Liu et al., 2009; Siegfried and Hothorn, 2020; Kowal and Wu, 2021). Suppose $\mathcal{A}_j = [a_j, a_{j+1})$ as in the examples above. The cumulative distribution functions of y and z are related as follows:

$$F_y(j) = \text{pr}(y \leq j) = \text{pr}\{z < g(a_{j+1})\} = F_z\{g(a_{j+1})\}. \quad (4)$$

By model (2), the latent z are Gaussian. Consider a working marginal distribution $z \sim N(\mu_z, \sigma_z^2)$, so $F_z(t) = \Phi\{(t - \mu_z)/\sigma_z\}$ for $t \in \mathbb{R}$. Rearranging (4) motivates the following estimator:

$$\hat{g}_0(a_{j+1}) = \bar{y} + \hat{s}_y \Phi^{-1}\{\tilde{F}_y(j)\} \quad (5)$$

along with the appropriate limiting behavior, i.e., $\hat{g}_0(-\infty) = -\infty$ and $\hat{g}_0(\infty) = \infty$. Since the transformation is identifiable only up to location (μ_z) and scale (σ_z), the estimator (5) matches the first two moments of z with those of y : $\mu_z = \bar{y}$ is the sample mean and $\sigma_z = \hat{s}_y$ is the sample standard deviation of $\{y_i\}_{i=1}^n$. Similarly, (5) substitutes a point estimate for F_y using the non-parametric estimator $\tilde{F}_y(j) = n(n+1)^{-1} \hat{F}_y(j)$ that rescales the empirical cumulative distribution function $\hat{F}_y(j) = n^{-1} \sum_{i=1}^n \mathbb{I}\{y_i \leq j\}$ to avoid boundary issues. Lastly, Kowal and Wu (2021) proposed a smooth interpolation of \hat{g}_0 on the observed values, $\hat{g}(y_i) = \hat{g}_0(y_i)$ for $i = 1, \dots, n$, where where \hat{g} is a monotonic cubic interpolating spline (Fritsch and Carlson, 1980). The limits of \hat{g}_0 are also imposed.

The distinction between \hat{g}_0 and \hat{g} highlights the importance of the rounding operator: \hat{g}_0 is a step function with $h \circ \hat{g}_0^{-1} = \hat{g}_0^{-1}$ and therefore does not need the rounding operator. However, the data-generating process of (1)–(2) with transformation \hat{g}_0 is supported only on the observed values: $\text{pr}(y = j) = 0$ whenever $g(a_j) = g(a_{j+1})$, which occurs for \hat{g}_0 when $j \notin \{y_i\}_{i=1}^n$. Instead, the smoothness of \hat{g} appropriately expands the support of the data-generating process, while the interpolation ensures that \hat{g} preserves (5) at the observed data values $\{y_i\}_{i=1}^n$.

Example 5. The estimator (5) may instead use parametric distributions, such as Poisson or Negative Binomial distribution functions. In this case, the role of the transformation is to map the latent data model (2) such that the marginal distribution of y conforms to a pre-specified parametric family. The accompanying parameters of F_y must be estimated; a useful default is method-of-moments estimation, which recycles \bar{y} and \hat{s}_y . Jia et al. (2021) adopted a related approach for count time series modeling, while Pitt et al. (2006) similarly used parametric regression models for the marginals in a multivariate Gaussian copula model.

Example 6. Semiparametric copula models similarly apply parametric or nonparametric estimates of F_y , but then define an extended rank (probit) likelihood that only uses the ordering of the data (Hoff, 2007; Feldman and Kowal, 2021). In particular, the ordering of $\{y_i\}$ imposes an equivalent ordering on $\{z_i\}$, which ensures that conditioning on the data is equivalent to applying a constraint region on z_i . This result is closely linked to the framework in the subsequent section.

2.2 Selection distributions

Under model (1)–(2), the likelihood for θ is

$$\text{pr}(y_i = j \mid \theta) = \text{pr}\{z_i \in g(\mathcal{A}_j) \mid \theta\} = \Pi_\theta\{g(\mathcal{A}_j) \mid x_i\} \quad (6)$$

with conditional independence across $i = 1, \dots, n$. Given a prior $p(\theta)$, the posterior distribution is

$$p(\theta | y) = \frac{p(\theta)\text{pr}\{z \in g(\mathcal{A}_y) | \theta\}}{\text{pr}\{z \in g(\mathcal{A}_y)\}} = \frac{p(\theta)\Pi_\theta\{g(\mathcal{A}_y) | x\}}{\int p(\theta)\Pi_\theta\{g(\mathcal{A}_y) | x\}d\theta} \quad (7)$$

where $\{z \in g(\mathcal{A}_y)\} = \{z_1 \in g(\mathcal{A}_{y_1}), \dots, z_n \in g(\mathcal{A}_{y_n})\}$ is elementwise.

Previous attempts at Bayesian modeling of (1)–(2) have applied Gibbs sampling algorithms for estimating functionals of (7) (Canale and Dunson, 2011, 2013; Kowal and Canale, 2020). The common strategy is to introduce a data-augmentation step in the Markov chain Monte Carlo algorithm and iteratively sample from $[z | y, \theta]$ and $[\theta | z, y] = [\theta | z]$. However, these Markov chain Monte Carlo algorithms fail to provide general insights about the posterior or predictive distribution under (1)–(2) and require customized diagnostics and lengthy simulation runs.

Here, we characterize the posterior distribution explicitly:

Theorem 1. *When $\mathcal{C} = g(\mathcal{A}_y)$ is a measurable subset of \mathbb{R}^n , the posterior distribution $p(\theta | y)$ under model (1)–(2) is a selection distribution.*

The result is self-evident from (6)–(7): a selection distribution is defined by random variables of the form $[\theta | z \in \mathcal{C}]$ and parametrized in terms of the joint distribution for (θ, z) and the measurable constraint region \mathcal{C} . Hence, the observation that $p(\theta | y) = p\{\theta | z \in g(\mathcal{A}_y)\}$ is sufficient.

General properties of selection distributions are provided by Arellano-Valle et al. (2006). When the prior $p(\theta)$ is closed under a set of transformations or closed under marginalization, these properties propagate to the posterior $p(\theta | y)$. When (θ, z) have a joint multivariate elliptically contoured distribution, the posterior density and distribution functions can be expressed in terms of the location parameters, dispersion parameters, and density generator function; see Arellano-Valle et al. (2006) for the explicit forms.

For a more tractable analysis, suppose that the prior $p(\theta)$ and the latent data model $\Pi_\theta(\cdot | x_i)$ are both Gaussian. Specifically, construct the joint distribution

$$\begin{pmatrix} z \\ \theta \end{pmatrix} \sim N_{n+p} \left\{ \begin{pmatrix} \mu_z \\ \mu_\theta \end{pmatrix}, \begin{pmatrix} \Sigma_z & \Sigma_{z\theta} \\ \Sigma'_{z\theta} & \Sigma_\theta \end{pmatrix} \right\} \quad (8)$$

for $z \in \mathbb{R}^n$ and $\theta \in \mathbb{R}^p$, where the moments may depend on the covariates $\{x_i\}_{i=1}^n$. Then the posterior may be characterized as follows:

Theorem 2. *Under the model (1) and (8), the posterior distribution is selection normal, denoted $[\theta | y] \sim \text{SLCT-}N_{n,p}(\mu_z, \mu_\theta, \Sigma_z, \Sigma_\theta, \Sigma_{z\theta}, \mathcal{C})$, with constraint region $\mathcal{C} = g(\mathcal{A}_y)$, density*

$$p(\theta | y) = \phi_p(\theta; \mu_\theta, \Sigma_\theta) \frac{\bar{\Phi}_n\{\mathcal{C}; \Sigma_{z\theta}\Sigma_\theta^{-1}(\theta - \mu_\theta) + \mu_z, \Sigma_z - \Sigma_{z\theta}\Sigma_\theta^{-1}\Sigma'_{z\theta}\}}{\bar{\Phi}_n(\mathcal{C}; \mu_z, \Sigma_z)}, \quad (9)$$

and moment generating function $M_{[\theta|z \in \mathcal{C}]}(s) = \exp(s'\mu_\theta + s'\Sigma_\theta s/2) \bar{\Phi}_n(\mathcal{C}; \Sigma_{z\theta}s + \mu_z, \Sigma_z) / \bar{\Phi}_n(\mathcal{C}; \mu_z, \Sigma_z)$, where $\phi_p(\cdot; \mu, \Sigma)$ denotes the Gaussian density function of a Gaussian random variable with mean μ and covariance Σ and $\bar{\Phi}_n(\mathcal{C}; \mu, \Sigma) = \int_{\mathcal{C}} \phi_n(x; \mu, \Sigma) dx$.

The posterior distribution is defined by the joint moments of (θ, z) in (8) and the constraint region implied by (1). Crucially, there exists a more constructive representation:

Theorem 3. *Let $V_0 \sim N_n(0, \Sigma_z)$ and $V_1 \sim N_p(0, \Sigma_\theta - \Sigma'_{z\theta} \Sigma_z^{-1} \Sigma_{z\theta})$ be independent with $V_0^{(\mathcal{C} - \mu_z)} = [V_0 \mid V_0 \in \mathcal{C} - \mu_z]$ for $\mathcal{C} = g(\mathcal{A}_y)$. Then $[\theta \mid y] = \mu_\theta + V_1 + \Sigma'_{z\theta} \Sigma_z^{-1} V_0^{(\mathcal{C} - \mu_z)}$.*

Most important, Theorem 3 enables direct Monte Carlo simulation from the posterior, rather than iterative Markov chain Monte Carlo. Specific examples are provided subsequently.

While simplifications are often available depending on the model form (see Sections 2.3 - 2.5), the primary computational bottleneck for evaluating the density (9) is the integration of an n -dimensional multivariate normal density, whereas the Monte Carlo sampler in Theorem 3 is limited by the draw from the n -dimensional truncated normal. Our computing strategies leverage recent algorithmic developments. In particular, Botev (2017) introduced a minimax exponential tilting strategy that accurately estimates the normalizing constant of a high-dimensional multivariate normal distribution and provides an efficient importance sampling algorithm for truncated multivariate normal variables with an accept-reject algorithm that achieves a high acceptance rate. These algorithms are efficient and accurate for moderate n , such as $n \approx 500$, and are implemented in the `TruncatedNormal` package in R.

As a secondary consequence of Theorem 3, the posterior mean and posterior variance of the regression coefficients are readily available:

$$E(\theta \mid y) = \mu_\theta + \Sigma'_{z\theta} \Sigma_z^{-1} E(V_0 \mid V_0 \in \mathcal{C} - \mu_z) \quad (10)$$

$$\text{var}(\theta \mid y) = \Sigma_\theta + \Sigma'_{z\theta} \Sigma_z^{-1} \{ \Sigma_z - \text{var}(V_0 \mid V_0 \in \mathcal{C} - \mu_z) \} \Sigma_z^{-1} \Sigma_{z\theta} \quad (11)$$

which depend on the moments of $V_0^{(\mathcal{C} - \mu_z)} = [V_0 \mid V_0 \in \mathcal{C} - \mu_z]$. These and other terms can be simplified depending on the model (8).

2.3 Posterior distribution for the linear model

Consider the linear model (3) with a Gaussian prior $\theta \sim N(\mu_\theta, \Sigma_\theta)$ and let $X = (x_1, \dots, x_n)'$ denote the $n \times p$ covariate matrix. The posterior distribution of the regression coefficients is available as a direct consequence of Theorem 2:

Lemma 1. *For model (1) and (3) with $\theta \sim N(\mu_\theta, \Sigma_\theta)$, the posterior distribution is $[\theta \mid y] \sim \text{SLCT-}N_{n,p}(\mu_z = X\mu_\theta, \mu_\theta, \Sigma_z = X\Sigma_\theta X' + \sigma^2 I_n, \Sigma_\theta, \Sigma_{z\theta} = X\Sigma_\theta, \mathcal{C} = g(\mathcal{A}_y))$.*

Lemma 1 enables evaluation of the posterior density (Theorem 2), direct Monte Carlo simulation from the posterior (Theorem 3), and computation of the posterior moments (equations (10) and (11)) for the linear model.

To obtain more analytically tractable posterior quantities, consider the g -prior (Zellner, 1986) for θ . Monte Carlo sampling from the posterior is simplified as follows:

Lemma 2. *Suppose $\Sigma_\theta = \psi \sigma^2 (X'X)^{-1}$ for $\psi > 0$. Under model (1) and (3), a posterior draw $\theta^* \sim p(\theta \mid y)$ is obtained as follows:*

1. Simulate $V_0^* \sim N_n(0, \sigma^2\{\psi X(X'X)^{-1}X' + I_n\})$ truncated to $g(\mathcal{A}_y) - X\mu_\theta$.
2. Simulate $V_1^* \sim N_p(0, \sigma^2\psi(1 + \psi)^{-1}(X'X)^{-1})$.
3. Set $\theta^* = \mu_\theta + V_1^* + \psi(1 + \psi)^{-1}(X'X)^{-1}X'V_0^*$.

Lemma 2 provides direct simulation from the posterior distribution of θ using standard regression functionals of X . Lemma 2 also simplifies the posterior expectation of the regression coefficients:

$$E(\theta | y) = \mu_\theta + \frac{\psi}{1 + \psi}(X'X)^{-1}X'\hat{z} \quad (12)$$

where $\hat{z} = E\{z | z \in g(\mathcal{A}_y) - X\mu_\theta\} = E(V_0^*)$ is the marginal expectation of z truncated to $g(\mathcal{A}_y) - X\mu_\theta$. Using Lemma 2, $E(\theta | y)$ is easily estimable by replacing \hat{z} with the sample mean of Monte Carlo draws of V_0^* . When the prior is centered at zero, $\mu_\theta = 0$ and $\hat{z} = E\{z | z \in g(\mathcal{A}_y)\} = E(z | y)$ is the posterior expectation of the latent data z unconditional on θ . By comparison, the zero-centered g -prior with a Gaussian likelihood for y produces a posterior expectation of the same form, but with the observed data y in place of \hat{z} . This comparison is particularly insightful in the context of the rounded data scenario from Example 1. In this case, z_i is the latent continuous version of the rounded data y_i , so $\hat{z}_i = E(z_i | y)$ is a reasonable proxy for the unobservable continuous data in the posterior expectation (12).

More broadly, Lemma 1 suggests a conjugate prior for model (1) and (3). In particular, the Gaussian distribution is a special case of the selection normal: $\theta \sim \text{SLCT-N}_{1,p}(\mu_z = 0, \mu_\theta, \Sigma_z = 1, \Sigma_\theta, \Sigma_{z\theta} = 0'_p, \mathcal{C} = \mathbb{R})$, where the moments and constraints on z are irrelevant as long as $\Sigma_{z\theta} = 0$. By generalizing these additional arguments, we obtain a richer class of conjugate priors:

Lemma 3. *Under the prior $\theta \sim \text{SLCT-N}_{n_0,p}(\mu_{z_0}, \mu_\theta, \Sigma_{z_0}, \Sigma_\theta, \Sigma_{z_0\theta}, \mathcal{C}_0)$ and the model (1) and (3), the posterior is $[\theta | y] \sim \text{SLCT-N}_{n_0+n,p}(\mu_{z_1}, \mu_\theta, \Sigma_{z_1}, \Sigma_\theta, \Sigma_{z_1\theta}, \mathcal{C}_1)$ with*

$$\mu_{z_1} = \begin{pmatrix} \mu_{z_0} \\ X\mu_\theta \end{pmatrix}, \quad \Sigma_{z_1} = \begin{pmatrix} \Sigma_{z_0} & \Sigma_{z_0\theta}X' \\ X\Sigma'_{z_0\theta} & X\Sigma_\theta X' + \sigma^2 I_n \end{pmatrix}, \quad \Sigma_{z_1\theta} = \begin{pmatrix} \Sigma_{z_0\theta} \\ X\Sigma_\theta \end{pmatrix}, \quad \mathcal{C}_1 = \mathcal{C}_0 \times g(\mathcal{A}_y).$$

Perhaps the most useful setting of Lemma 3 is sequential updating based on multiple datasets, say $y^{(1)}$ and $y^{(2)}$. When these datasets are conditionally independent and follow the same model (1) and (3), the total posterior decomposes as $p(\theta | y^{(1)}, y^{(2)}) \propto p(\theta | y^{(1)})p(y^{(2)} | \theta)$. Under a Gaussian prior for $p(\theta)$, Lemma 1 implies that the partial posterior $p(\theta | y^{(1)})$ is selection normal, which serves as the prior for the second dataset update. Hence, Lemma 3 provides the direct updates from the partial posterior $p(\theta | y^{(1)})$ to the total posterior $p(\theta | y^{(1)}, y^{(2)})$.

2.4 Prediction

A crucial feature of the model (1)–(2) is that the data-generating process and therefore the predictive distribution is discrete and matches the support of y . Consider the posterior predictive distribution at the $\tilde{n} \times p$ covariate matrix $\tilde{X} = (\tilde{x}_1, \dots, \tilde{x}_{\tilde{n}})'$. Because of the link in (1), the joint predictive distribution of $\tilde{y} = (\tilde{y}_1, \dots, \tilde{y}_{\tilde{n}})'$ can be expressed via the latent variables \tilde{z} :

$$\text{pr}(\tilde{y} | y) = \text{pr}\{\tilde{z} \in g(\mathcal{A}_{\tilde{y}}) | y\} = \int \text{pr}\{\tilde{z} \in g(\mathcal{A}_{\tilde{y}}) | \theta\}p(\theta | y)d\theta. \quad (13)$$

We consider multiple computing strategies for (functionals of) the posterior predictive distribution. The simplest option is to leverage the Monte Carlo sampling algorithms for $p(\theta | y)$ (e.g., Theorem 3) to obtain latent predictive samples from $[\tilde{z} | y]$, and then map those to \tilde{y} via (1):

Lemma 4. *A predictive draw $\tilde{y}^* \sim p(\tilde{y} | y)$ for model (1)–(2) is generated as follows: sample $\theta^* \sim p(\theta | y)$; sample $\tilde{z}^* \sim \Pi_{\theta=\theta^*}(\cdot | \tilde{X})$; set $\tilde{y}^* = h \circ g^{-1}(\tilde{z}^*)$.*

The result is a direct consequence of the conditional independence assumptions in (2) and the deterministic link in (1). The samples are discrete to match the support of y and capture the joint dependence among predictive variables at multiple covariates \tilde{X} . For the linear model (3), the posterior sampling step is available via Monte Carlo sampling (e.g., Lemma 2). As a result, Lemma 4 produces Monte Carlo samples from the joint posterior predictive distribution. The latent predictive step is simply $\tilde{z}^* \sim N_{\tilde{n}}(\tilde{X}\theta^*, \sigma^2 I_{\tilde{n}})$, so Lemma 4 requires minimal additional computational cost given $\theta^* \sim p(\theta | y)$.

An alternative Monte Carlo sampler for the linear model circumvents the posterior sampling and instead draws directly from the latent posterior predictive distribution of $[\tilde{z} | y]$, which can be derived explicitly:

Lemma 5. *For the linear model (3) with a Gaussian prior $\theta \sim N(\mu_\theta, \Sigma_\theta)$, the latent predictive distribution at \tilde{X} is $[\tilde{z} | y] \sim \text{SLCT-}N_{n, \tilde{n}}(X\mu_\theta, \tilde{X}\mu_\theta, X\Sigma_\theta X' + \sigma^2 I_n, \tilde{X}\Sigma_\theta \tilde{X}' + \sigma^2 I_{\tilde{n}}, X\Sigma_\theta \tilde{X}', \mathcal{C} = g(\mathcal{A}_y))$.*

Direct Monte Carlo simulation proceeds using Theorem 3 applied to the latent predictive selection normal distribution, which we simplify for the g -prior:

Lemma 6. *Suppose $\Sigma_\theta = \psi\sigma^2(X'X)^{-1}$ for $\psi > 0$. Under model (1) and (3), a joint predictive draw $\tilde{y}^* \sim p(\tilde{y} | y)$ at the $\tilde{n} \times p$ covariate matrix \tilde{X} is obtained as follows:*

1. Simulate $V_0^* \sim N_n(0, \sigma^2\{\psi X(X'X)^{-1}X' + I_n\})$ truncated to $g(\mathcal{A}_y) - X\mu_\theta$.
2. Simulate $\tilde{V}_1^* \sim N_{\tilde{n}}(0, \sigma^2\{\psi(1 + \psi)^{-1}\tilde{X}(X'X)^{-1}\tilde{X}' + I_{\tilde{n}}\})$.
3. Compute $\tilde{z}^* = \tilde{X}\mu_\theta + \tilde{V}_1^* + \psi(1 + \psi)^{-1}\tilde{X}(X'X)^{-1}X'V_0^*$.
4. Set $\tilde{y}^* = h \circ g^{-1}(\tilde{z}^*)$.

Lemma 6 provides direct Monte Carlo sampling from the joint posterior predictive distribution using standard regression functionals of the covariate matrix X and the predictive covariate matrix \tilde{X} . By comparison, the samplers in Lemma 2 and Lemma 6 share the same simulation step for V_0^* , but the second step differs: Lemma 2 requires a draw from a p -dimensional multivariate normal distribution, while Lemma 6 draws from a \tilde{n} -dimensional multivariate normal distribution. As a result, Lemma 6 may provide computational savings relative to Lemma 4 when \tilde{n} is small, p is large, and the posterior samples of θ are not needed.

Analytic computations for predictive inference that avoid Monte Carlo sampling are also available. The predictive distribution is computable using the marginal density of (1) and (3):

$$\text{pr}(\tilde{y} | y) = \text{pr}(\tilde{y}, y) / \text{pr}(y). \quad (14)$$

The marginal distribution is the constant term in the denominator of (9),

$$\text{pr}(y) = \bar{\Phi}_n\{\mathcal{C} = g(\mathcal{A}_y); \mu_z, \Sigma_z\}, \quad (15)$$

where μ_z and Σ_z are determined by the model (2), e.g., $\mu_z = X\mu_\theta$ and $\Sigma_z = X\Sigma_\theta X' + \sigma^2 I_n$ in the linear model setting of Lemma 1. The joint distribution $\text{pr}(\tilde{y}, y)$ proceeds similarly via the latent data (\tilde{z}, z) : $\text{pr}(\tilde{y}, y) = \bar{\Phi}_{n+\tilde{n}}\{\mathcal{C} = g(\mathcal{A}_{\tilde{y}}) \times g(\mathcal{A}_y); \mu_{\tilde{z}z}, \Sigma_{\tilde{z}z}\}$, where

$$\mu_{\tilde{z}z} = \begin{pmatrix} \tilde{X}\mu_\theta \\ X\mu_\theta \end{pmatrix}, \quad \Sigma_{\tilde{z}z} = \begin{pmatrix} \tilde{X}\Sigma_\theta\tilde{X}' + \sigma^2 I_{\tilde{n}} & \tilde{X}\Sigma_\theta X' \\ X\Sigma_\theta\tilde{X}' & X\Sigma_\theta X' + \sigma^2 I_n \end{pmatrix}$$

for the linear model setting of Lemma 1. These direct probability computations of $\text{pr}(\tilde{y} \mid y)$ are most useful when \tilde{n} is small, such as $\tilde{n} = 1$.

Lastly, the predictive probabilities provide analytic point predictions, such as $E(\tilde{y} \mid y) = \sum_{j \in \text{supp}(y)} j \text{pr}(\tilde{y} = j \mid y)$. When $\text{supp}(y) = \mathbb{Z}$ or is large, these predictive probability evaluations may be computationally prohibitive. In that case, the Monte Carlo simulation is a more appealing option for computing predictive moments and other functionals.

2.5 Nonlinear basis regression

The linear model (3) can accommodate nonlinear regressions via basis expansions. Consider modeling $z_i = z(\tau_i)$ as a smooth function of τ with the following adaptation of (3):

$$z_i = b'(\tau_i)\theta + \epsilon_i, \quad \epsilon_i \sim N(0, \sigma^2) \quad (16)$$

where $b'(\tau) = (b_1(\tau), \dots, b_p(\tau))$ is a vector of known basis functions, such as splines, Fourier functions, or wavelets. Canale and Dunson (2011) applied a version of model (16) for count data analysis, but required a Markov chain Monte Carlo algorithm for posterior inference.

Let $X = (b(\tau_1), \dots, b(\tau_n))'$ denote the basis matrix. Basis expansions such as (16) are usually accompanied by a smoothness prior of the form $\theta \sim N_p(0, \psi\sigma^2\Omega^-)$, where $\psi > 0$ controls the smoothness and Ω is a known positive semidefinite penalty matrix. For common choices of Ω , Scheipl et al. (2012) showed that X and Ω can be reparametrized such that the distribution of $X\theta$ is unchanged, but $\Omega = I_p$ is the identity and $X'X$ is diagonal. Hence, we proceed under the assumption that $X'X = \text{diag}\{d_j\}$ and $\theta \sim N_p(0, \psi\sigma^2 I_p)$.

We focus on the predictive distribution $\text{pr}\{\tilde{y}(\tau) \mid y\}$ across multiple points τ . Monte Carlo simulation proceeds directly without requiring samples from the posterior:

Lemma 7. *Suppose $\theta \sim N_p(0, \psi\sigma^2 I_p)$ for $\psi > 0$ and $X'X = \text{diag}\{d_j\}$. Under model (1) and (16), a joint predictive draw $\tilde{y}^* \sim p(\tilde{y} \mid y)$ at the observation points $\tau_{1'}, \dots, \tau_{\tilde{n}'}$ with $\tilde{X} = (b(\tau_{1'}), \dots, b(\tau_{\tilde{n}'}))'$ is obtained as follows:*

1. Simulate $V_0^* \sim N_n(0, \sigma^2(\psi X X' + I_n))$ truncated to $g(\mathcal{A}_y)$.
2. Simulate $\tilde{V}_1^* \sim N_{\tilde{n}}(0, \sigma^2[\psi \tilde{X} \text{diag}\{1/(1 + \psi d_j)\} \tilde{X}' + I_{\tilde{n}}])$.
3. Compute $\tilde{z}^* = \tilde{V}_1^* + \psi \tilde{X} \text{diag}\{1 - \psi d_j/(1 + \psi d_j)\} \tilde{X}' V_0^*$.

4. Set $\tilde{y}^* = h \circ g^{-1}(\tilde{z}^*)$.

Lemma 7 provides Monte Carlo simulation from the joint predictive distribution of a discrete and nonlinear regression model. Most notably, the key terms are computable without any matrix inversions. The most demanding step is again the simulation of V_0^* from the n -dimensional truncated normal. Fortunately, this draw is shared among all choices of points $\tau_{1'}, \dots, \tau_{\tilde{n}'}$.

More broadly, Lemma 7 is applicable for predictive simulation from any linear model (1) and (3) with a prior of the form $\theta \sim N_p(0, \psi\sigma^2\Omega^-)$ for a known positive semidefinite matrix Ω . Although the reparametrization of $X\theta$ changes the interpretation of X and θ , it does not change the data-generating process, so the predictive draws remain valid.

2.6 Model and variable selection

Suppose we have candidate models $\mathcal{M}_1, \dots, \mathcal{M}_K$, where each \mathcal{M}_k is of the form (1)–(2). Each candidate model differs in a fixed attribute: examples include the transformation g , the hyperparameters in the model (such as ψ), and linear (3) against nonlinear (16) models. This setting also applies to variable selection by replacing each covariate matrix X with X_γ , where $\gamma \in \{0, 1\}^p$ is a variable inclusion indicator and each γ corresponds to a model \mathcal{M}_k . We focus on two goals: model selection and prediction via model-averaging.

Given model probabilities $\text{pr}(\mathcal{M}_k)$ for $k = 1, \dots, K$, the posterior probability of each model is

$$\text{pr}(\mathcal{M}_k | y) = \frac{\text{pr}(y | \mathcal{M}_k)\text{pr}(\mathcal{M}_k)}{\sum_{h=1}^K \text{pr}(y | \mathcal{M}_h)\text{pr}(\mathcal{M}_h)} \quad (17)$$

where $\text{pr}(y | \mathcal{M}_k)$ denotes the marginal likelihood under \mathcal{M}_k . When the prior on θ and the latent continuous data model for z are both Gaussian in the form of (8) for each \mathcal{M}_k , we derive the posterior probabilities directly:

Lemma 8. *For each model $\{\mathcal{M}_k\}_{k=1}^K$ of the form (1)–(2) with transformation $g^{(k)}$, suppose that $(\theta^{(k)}, z^{(k)})$ are jointly Gaussian with $z^{(k)} \sim N_n(\mu_z^{(k)}, \Sigma_z^{(k)})$. Then the posterior model probabilities are*

$$\text{pr}(\mathcal{M}_k | y) = \frac{\bar{\Phi}_n\{\mathcal{C} = g^{(k)}(\mathcal{A}_y); \mu_z^{(k)}, \Sigma_z^{(k)}\}\text{pr}(\mathcal{M}_k)}{\sum_{h=1}^K \bar{\Phi}_n\{\mathcal{C} = g^{(h)}(\mathcal{A}_y); \mu_z^{(h)}, \Sigma_z^{(h)}\}\text{pr}(\mathcal{M}_h)}. \quad (18)$$

Lemma 8 is naturally informative for model selection, for example by selecting \mathcal{M}_k for which $\text{pr}(\mathcal{M}_k | y)$ is largest. More broadly, the posterior probabilities in (18) enable model uncertainty in posterior and predictive inference. Focusing on the latter setting, consider the goal of prediction that averages over the uncertainty about the models $\{\mathcal{M}_k\}_{k=1}^K$. Using the predictive simulators, which now depend on the specific model \mathcal{M}_k , we propose the following Monte Carlo sampler: for $s = 1, \dots, S$, sample $k^s \sim \text{Categorical}(\pi_1, \dots, \pi_K)$ with $\pi_k = \text{pr}(\mathcal{M}_k | y)$ from (18); then sample $\tilde{y}^s \sim \text{pr}(\tilde{y} | y, \mathcal{M} = \mathcal{M}_{k^s})$ from Lemma 4. This sampler produces joint and independent draws of $\{(\mathcal{M}^s, \tilde{y}^s)\}_{s=1}^S \sim \text{pr}(\mathcal{M}, \tilde{y} | y)$. By computing functionals of $\{\tilde{y}^s\}$ only, we effectively marginalize over the model uncertainty within $\{\mathcal{M}_k\}_{k=1}^K$ yet retain a discrete and joint predictive distribution at \tilde{X} .

2.7 The sparse means problem for discrete data

The classical sparse means problem considers continuous data $[z_i | \theta_i] \sim N(\theta_i, \sigma^2)$ with the goal of identifying the nonzero means, $\{i : \theta_i \neq 0\}$ (Castillo and van der Vaart, 2012). Instead, suppose we observe discrete data $y_i \in \mathbb{Z}$ under model (1)–(2). In the context of Example 1, this scenario corresponds to the normal means model for rounded data. We introduce sparsity in $\{\theta_i\}_{i=1}^n$ via the spike-and-slab model

$$[\theta_i | \gamma_i] \sim \gamma_i N(0, \sigma^2 \psi) + (1 - \gamma_i) \delta_{\{0\}} \quad (19)$$

where $\gamma_i \in \{0, 1\}$ is the inclusion indicator with $\text{pr}(\gamma_i = 1 | \pi) = \pi$. Conditional on the inclusion indicators, this model is a special case of (3) with $X = I_n$ and $n = p$, where the prior for the active components $[\theta_i | \gamma_i = 1] \sim N(0, \sigma^2 \psi)$ is a special case of the Gaussian priors considered previously. This scenario is also useful for wavelet models and can be extended to other spike-and-slab priors.

The sparse means model with prior (19) offers certain computational simplifications, but also introduces new challenges. In particular, inference on the inclusion indicators $[\gamma | y]$ proceeds via Lemma 8. Since the marginal latent mean is zero and the latent covariance is diagonal, $\Sigma_z^{(\gamma)} = \sigma^2 \text{diag}\{1 + \psi \gamma_i\}_{i=1}^n$, the key term in (18) simplifies considerably:

$$\bar{\Phi}_n\{\mathcal{C} = g(\mathcal{A}_y); 0, \Sigma_z^{(\gamma)}\} = \prod_{i=1}^n \int_{g(y_i-0.5)}^{g(y_i+0.5)} \phi_1\{x_i; 0, \sigma^2(1 + \psi \gamma_i)\} dx_i. \quad (20)$$

In place of an n -dimensional integral of a multivariate normal density, we obtain a product of n univariate normal integrals, which is a massive advantage for computing with large n .

Despite these gains for evaluating each $\text{pr}(\gamma | y)$, the search over the model space requires consideration of 2^n models, which is computationally prohibitive even for moderate n . Instead, we may employ a stochastic search to sample from $[\gamma | y]$. Specifically, we apply a Gibbs sampler that cycles through $[\gamma_i | y, \gamma_{-i}]$ for $i = 1, \dots, n$, which observes that $\text{pr}(\gamma_i = 1 | y, \gamma_{-i}) = \omega_i / (1 + \omega_i)$ for the (full conditional) odds of inclusion

$$\omega_i = \frac{\text{pr}(\gamma_i = 1 | y, \gamma_{-i})}{\text{pr}(\gamma_i = 0 | y, \gamma_{-i})} = \frac{\pi}{1 - \pi} \frac{\text{pr}(y | \gamma_{-i}, \gamma_i = 1)}{\text{pr}(y | \gamma_{-i}, \gamma_i = 0)} \quad (21)$$

where the terms of the form $\text{pr}(y | \gamma)$ are given by (20). We may expand this Gibbs sampler to incorporate a prior on the inclusion probability, $\pi \sim \text{Beta}(a_\pi, b_\pi)$ (Scott and Berger, 2010), which adds a simple sampling step of the form $[\pi | \gamma] \sim \text{Beta}(a_\pi + \#\{\gamma_i = 1\}, b_\pi + \#\{\gamma_i = 0\})$ with an accompanying update for π in (21) at each Gibbs sweep of $\gamma_1, \dots, \gamma_n, \pi$.

Inference on the regression coefficients θ is readily available by observing that $[\theta, \gamma | y] = [\theta | y, \gamma][\gamma | y]$. Given samples of γ using the above procedure, we sample from $[\theta | y, \gamma]$ using the following fast version of Lemma 2: for $\{i : \gamma_i = 1\}$, sample $V_{0,i}^* \sim N\{0, \sigma^2(1 + \psi)\}$ truncated to $[g(y_i - 0.5), g(y_i + 0.5)]$; sample $V_{1,i}^* \sim N\{0, \sigma^2 \psi(1 + \psi)^{-1}\}$; and set $\theta_i^* = V_{1,i}^* + \psi(1 + \psi)^{-1} V_{0,i}^*$. We set $\theta_i^* = 0$ for all $\{i : \gamma_i = 0\}$. This sampler is parallelizable across $i = 1, \dots, n$ yet produces draws from the joint posterior of θ . The draws of θ are not needed for sampling the inclusion indicators γ , but can be used to obtain predictive samples by application of Lemma 4.

3 Empirical results

3.1 Direct Monte Carlo and Gibbs sampling

To demonstrate the computational advantages of direct Monte Carlo sampling for posterior inference, we compare the proposed sampler from Lemma 2 with the Gibbs sampler from Kowal and Canale (2020). The two samplers are applied to the same linear regression model (3) with a g -prior (see Lemma 2). We fix σ at the maximum likelihood estimator (Kowal and Wu, 2021) and set $\psi = 1000$. The transformation and rounding operators for (1) are given by Example 2 with $y_{max} = \infty$ and Example 4, respectively.

We simulate negative binomial count data with independent Gaussian covariates using the design from Kowal and Canale (2020). The focus here is exclusively on computational performance. For varying sample sizes $n \in \{100, 200, 500\}$ and number of covariates $p \in \{10, 50\}$, we run each algorithm for 1000 samples (after a burn-in of 1000 for the Gibbs sampler).

For each simulation, we compute the median effective sample size across the regression coefficients $\{\theta_j\}_{j=1}^p$ and report the result as the percent of the total number of simulations (1000). In addition, we record the raw computing time (using R on a MacBook Pro, 2.8 GHz Intel Core i7). The results are presented in Figure 1. Most notably, the proposed Monte Carlo sampler achieves maximal efficiency for all n, p considered. By comparison, the Gibbs sampler produces 40-70% efficiency for $p = 10$, but the efficiency declines as p increases, including only 5-20% efficiency for $n = 100, p = 50$. In addition, the raw computing times are comparable for $n \in \{100, 200\}$ regardless of p , while the proposed Monte Carlo sampler incurs some additional cost only for $n = 500$. In general, the proposed Monte Carlo sampler demonstrates substantial efficiency gains with increasing p , especially when n is moderate.

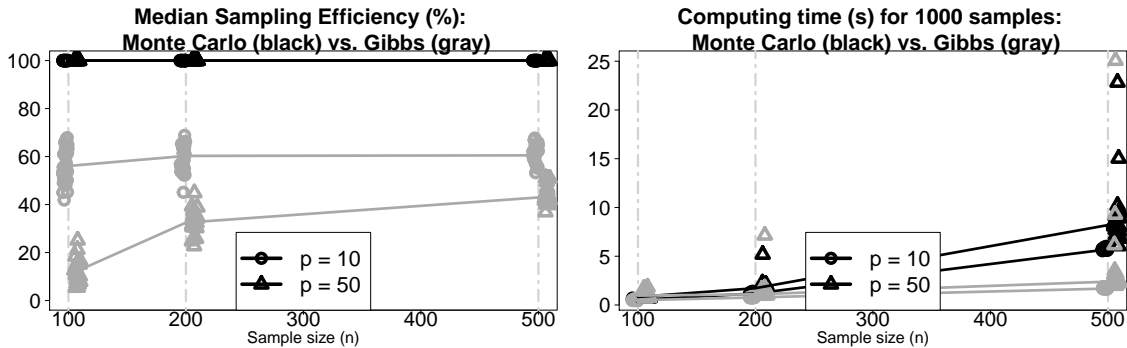


Figure 1: Median effective sample size across $\{\theta_j\}_{j=1}^p$ reported as the percent of the total number of simulations (left) and raw computing time for 1000 samples (right). Results are computed for 25 synthetic datasets (jittered points) and summarized using medians (non-vertical lines) with $n \in \{100, 200, 500\}$ and $p \in \{10, 50\}$.

3.2 Prediction for nonlinear regression with synthetic data

We evaluate the predictive distributions from count-valued nonlinear regression models using simulated data. We consider two data-generating processes: one with a Negative Binomial likelihood (Neg-Bin) and one that resembles (1) and (16) (Mixture-CDF). In both cases, we generate a latent smooth curve $f_{true}(\tau) = \sum_{j=1}^4 f_j(\tau)\beta_j$ on a grid of $n = 250$ points, where $\{f_j\}$ are orthonormal polynomials of degree j and $\{\beta_j\}$ are independent normal variables with mean zero and decreasing variance $4 - j + 1$. For the Negative Binomial case, we set the mean function to be $\exp\{f_{true}(\tau)\}$ and the dispersion to be 10, which produces moderately overdispersed counts. We bound these data at $y_{max} = 30$ to prevent exceedingly large values. For the second case, we specify the rounding operator as in Example 2 with $y_{max} = 30$. The transformation is defined akin to Examples 4 or 5: we smooth the distribution function of a random variable that places 1/2 mass on a Poisson(10) distribution, 1/4 mass uniformly on the set of heaps $\{5, 10, \dots, 25\}$, and 1/4 mass uniformly on the set of boundaries $\{0, 30\}$. The data-generating model (16) is completed by setting f_{true} to be the mean of the latent data and $\sigma = 0.7$. The simulations are repeated for 100 iterations in each case.

Monte Carlo samples from the predictive distribution under model (1) and (16) are generated according to Lemma 7 for the following transformations: identity, square-root, and log (see Example 3); the empirical cumulative distribution function transformation (see Example 4); and the Poisson- and Negative Binomial-based parametric transformations (see Example 5). In each case, we set $\psi = 1000$ and estimate σ using the maximum likelihood estimator. In addition, we compute the predictive distribution from a model-averaged version of all of these transformations (with equal prior weights) using the sampler following Lemma 8. To streamline the results, only a subset of the transformations are presented, yet all are included in the model averaging. For benchmarking, we include Poisson and Negative Binomial spline regression models implemented in `stan_gamm4` in the `rstanarm` package in R using the default specifications.

The predictive distributions are evaluated using ranked probability scores, which is a proper scoring rule for discrete data predictive distributions (Czado et al., 2009). In addition, we compute mean interval width and empirical coverage (on out-of-sample testing points) for 90% pointwise prediction intervals. The results are presented in Figure 2.

For the Negative Binomial setting, the predictive distributions all perform similarly, with the proposed model-averaged predictions offering slight improvements over the fixed transformations. The prediction intervals are all conservative, with the surprising result that the Negative Binomial-based parametric transformation within the proposed framework offers narrower intervals than the Negative Binomial model, even though the latter model is a direct match for the data-generating process. One plausible reason is the computational challenges of the Negative Binomial sampler: it is difficult to learn both the dispersion parameter and the nonlinear mean function, and the output from `stan_gamm4` regularly reports low effective sample sizes.

For the second case, the gains of the proposed strategy are now more apparent: the ranked probability scores especially favor the nonparametric transformation (Example 4) and the model-averaged predictions. The prediction intervals confirm these advantages, with an additional warning regarding the Poisson model: the intervals remain narrower as in the previous case, but the empirical coverage is now far below the nominal 90%. Again the nonparametric transformation

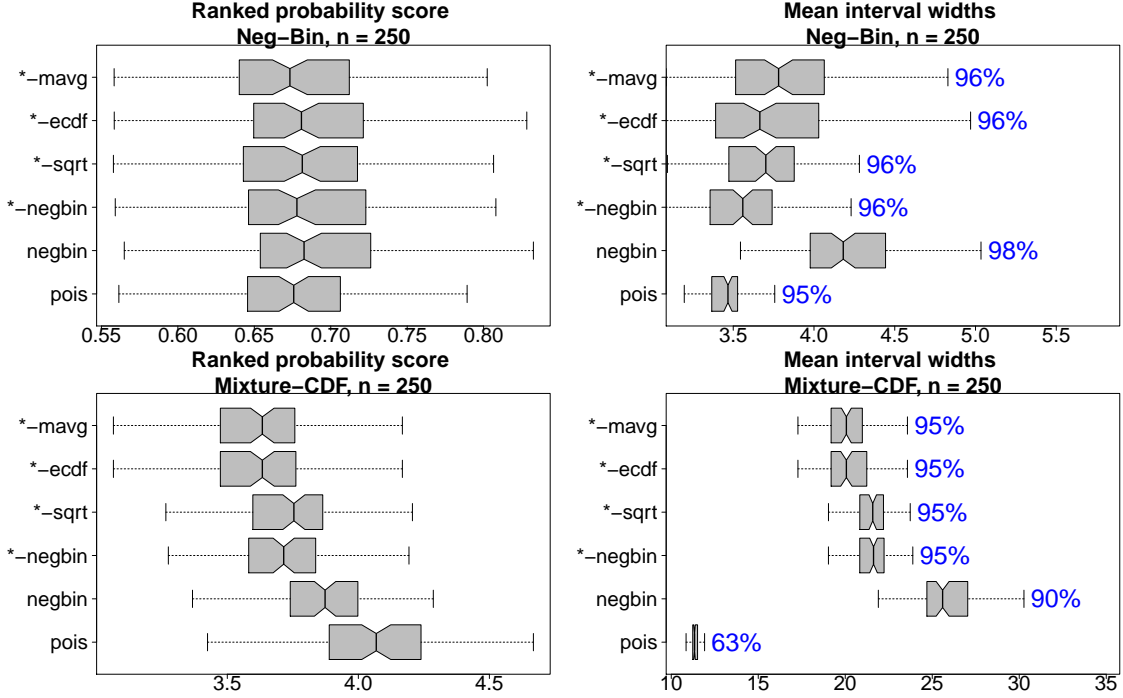


Figure 2: Ranked probability score (left) and mean prediction interval widths with empirical coverage (right) for Negative Binomial data (top) and Mixture-CDF data (bottom); proposed methods are denoted (*).

and the model-averaged predictions perform similarly: the model probabilities place nearly all of the weight on the nonparametric transformation, so this result is consistent.

3.3 Sparse means estimation for synthetic rounded data

Lastly, we evaluate the selection capabilities of the sparse means model under rounding. The goal is to assess (i) whether an omission of the rounding operator impacts selection ability and (ii) whether the transformation is helpful for this task. Synthetic rounded data are generated as $y_i = \lfloor z_i \rfloor$ with $z_i = \theta_i + \epsilon_i$ and $\epsilon_i \sim N(0, 1)$, where $\theta_i = \mu\gamma_i$ and μ denotes the signal strength with variable inclusion indicator $\gamma_i \in \{0, 1\}$. We use a small or moderate proportion of signals, $\#\{\gamma_i = 1\}/n \in \{0.1, 0.5\}$. Results are presented for $\mu = 2$ and $n = 200$; increasing $\mu \geq 3$ uniformly improved results and $n = 500$ produced similar conclusions.

For all competing methods, we apply the same sparsity prior (19) accompanied by $\pi \sim \text{Beta}(1, 1)$ and $\psi^{1/2} \sim \text{Uniform}(0, n^{1/2})$. We include two variations of the proposed approach, both with the rounding operator from Example 1: one uses the identity transformation (as in the data-generating process) and the other uses the empirical cumulative distribution function transformation (see Example 4). In addition, we include a Gaussian model that omits the rounding operation entirely. To maintain focus on the modeling specifications, we apply identical Gibbs sampling strategies as outlined in Section 2.7; the Gaussian case simply replaces (21) with the relevant Gaussian likelihoods. The additional Gibbs sampling step for all models is $[\psi^{-1} \mid y, \theta, \gamma] \sim \text{Gamma}\{\#\{\gamma_i =$

$1\}/2 - 1/2, \sum_{i:\gamma_i=1} \theta_i^2/(2\sigma^2)\}$ truncated to $[1/n, \infty)$. Lastly, we fix σ at the the maximum likelihood estimator from a `kmeans` model with two clusters.

The primary inferential target is $\text{pr}(\gamma_i = 1 \mid y)$, which we use to select the nonzero means. The receiving operator characteristic curves for this selection mechanism (averaged over 100 simulations) and the corresponding area under the curve values (presented across 100 simulations) are in Figure 3. Perhaps most surprising, the nonparametric transformation from Example 4 provides the best selection capabilities by a wide margin. Comparing the identity models with and without rounding, we find that the rounding operator offers only minor advantages for selection. Nonetheless, the best performer belongs to the proposed modeling class (1)–(2), which is a coherent data-generating process for the discrete (rounded) data.

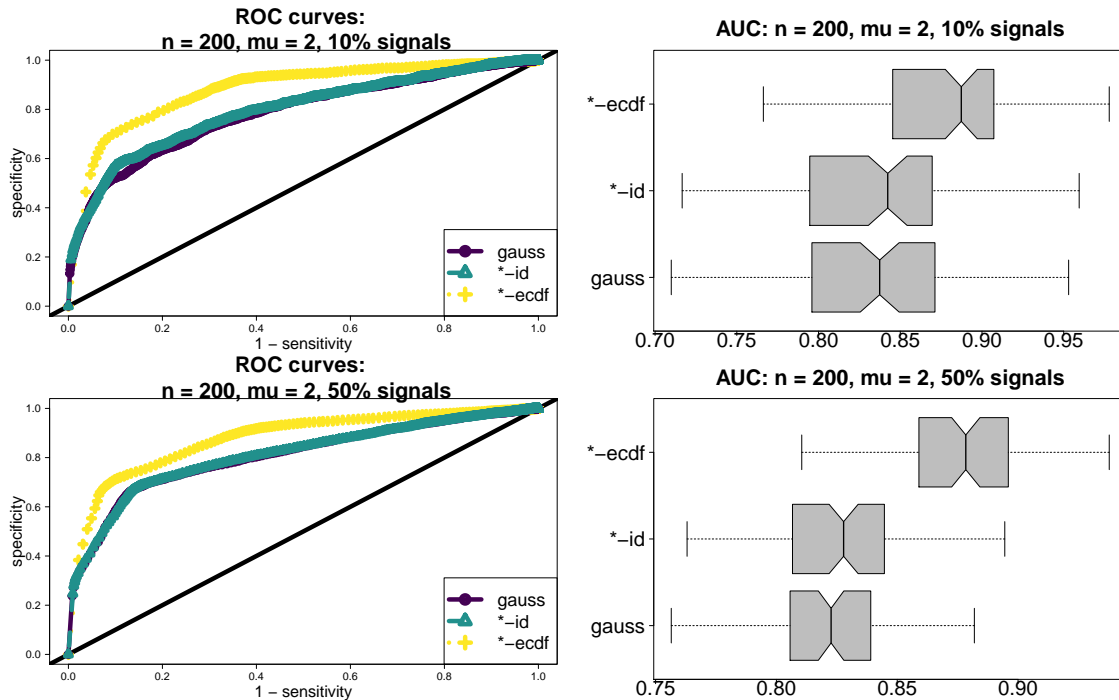


Figure 3: Receiver operating characteristic curve (left) and corresponding area under the curve (right) for sparse means selection with rounded data; proposed methods are denoted (*).

4 Discussion

Despite the generality of the linear model (1) and (3), the posterior and predictive derivations treat the variance components as known. Our analyses estimate σ using maximum likelihood, although other estimators are available. Alternatively, we may place a prior on σ and marginalize over this unknown parameter. When σ^2 is assigned an inverse-Gamma prior, the joint distribution of (θ, z) as in (8), but unconditional on σ^2 , is a multivariate *t*-distribution. The posterior distribution $p(\theta \mid y)$ is therefore a *selection t-distribution*, for which the density and distribution functions are given in Arellano-Valle et al. (2006).

For more general regression scenarios with $\epsilon \sim N_n(0, \Sigma_\epsilon)$ or with hyperpriors on $(\mu_\theta, \Sigma_\theta)$ such as for hierarchical modeling, the posterior derivations remain relevant and provide a blocked Gibbs sampling strategy. Let $\Sigma = (\Sigma_\epsilon, \mu_\theta, \Sigma_\theta)$ denote the parameters excluding θ . A blocked Gibbs sampler proceeds iteratively by drawing $[z, \theta | y, \Sigma] = [\theta | y, \Sigma][z | y, \theta, \Sigma]$ and $[\Sigma | y, z, \theta]$. The first block uses the selection normal posterior for θ , while $[z | y, \theta, \Sigma] \sim N_n(X\theta, \Sigma_\epsilon)$ truncated to $g(\mathcal{A}_y)$. When Σ_ϵ is diagonal, this step only requires n draws from independent and univariate truncated normals, which does not add much computational cost. The remaining block typically satisfies $[\Sigma | y, z, \theta] = [\Sigma | z, \theta]$ and therefore may use existing sampling steps for variance parameters in (continuous) Gaussian models. Importantly, our selection normal results provide a joint sampling step for $[z, \theta | y, \Sigma]$, which protects against Markov chain Monte Carlo sampling inefficiencies due to posterior correlations among z and θ .

In concurrent research, King and Kowal (2021) introduce a dynamic linear model in (2) for count time series data, which extends the dynamic probit results of Fasano et al. (2021). The conjugacy afforded by Lemma 3 enables analytic recursions for filtering and smoothing (selection normal) distributions, which are accompanied by an optimal particle filter for online inference. Similar conjugacy results and computational advantages may be available for spatial, functional, or other dependent integer-valued data.

References

- Arellano-Valle, R. B., Branco, M. D., and Genton, M. G. (2006). A unified view on skewed distributions arising from selections. *Canadian Journal of Statistics*, 34(4):581–601.
- Botev, Z. I. (2017). The normal law under linear restrictions: simulation and estimation via minimax tilting. *Journal of the Royal Statistical Society. Series B: Statistical Methodology*, 79(1):125–148.
- Box, G. E. P. and Cox, D. R. (1964). An analysis of transformations. *Journal of the Royal Statistical Society: Series B (Methodological)*, 26(2):211–243.
- Bradley, J. R., Holan, S. H., and Wikle, C. K. (2018). Computationally efficient multivariate spatio-temporal models for high-dimensional count-valued data (with discussion). *Bayesian Analysis*, 13(1):253–310.
- Canale, A. and Dunson, D. B. (2011). Bayesian kernel mixtures for counts. *Journal of the American Statistical Association*, 106(496):1528–1539.
- Canale, A. and Dunson, D. B. (2013). Nonparametric Bayes modelling of count processes. *Biometrika*, 100(4):801–816.
- Castillo, I. and van der Vaart, A. (2012). Needles and straw in a haystack: Posterior concentration for possibly sparse sequences. *The Annals of Statistics*, 40(4):2069–2101.
- Czado, C., Gneiting, T., and Held, L. (2009). Predictive model assessment for count data. *Biometrics*, 65(4):1254–1261.

- Dempster, A. P. and Rubin, D. B. (1983). Rounding error in regression: The appropriateness of Sheppard's corrections. *Journal of the Royal Statistical Society: Series B (Methodological)*, 45(1):51–59.
- Durante, D. (2019). Conjugate Bayes for probit regression via unified skew-normal distributions. *Biometrika*, 106(4):765–779.
- Fasano, A. and Durante, D. (2020). A class of conjugate priors for multinomial probit models which includes the multivariate normal one. *arXiv preprint arXiv:2007.06944*.
- Fasano, A., Rebaudo, G., Durante, D., and Petrone, S. (2021). A closed-form filter for binary time series. *Statistics and Computing*, 31(4):1–20.
- Feldman, J. and Kowal, D. (2021). A Bayesian Framework for Generation of Fully Synthetic Mixed Datasets. *Annals of Applied Statistics (revision submitted)*.
- Fritsch, F. N. and Carlson, R. E. (1980). Monotone piecewise cubic interpolation. *SIAM Journal on Numerical Analysis*, 17(2):238–246.
- Heitjan, D. F. (1989). Inference from grouped continuous data: a review. *Statistical science*, 4(2):164–179.
- Heitjan, D. F. and Rubin, D. B. (1991). Ignorability and coarse data. *The annals of statistics*, pages 2244–2253.
- Hoff, P. D. (2007). Extending the rank likelihood for semiparametric copula estimation. *The Annals of Applied Statistics*, 1(1):265–283.
- Jia, Y., Kechagias, S., Livsey, J., Lund, R., and Pipiras, V. (2021). Latent Gaussian Count Time Series. *Journal of the American Statistical Association*, (just-accepted):1–28.
- King, B. and Kowal, D. R. (2021). Warped Dynamic Linear Models for Time Series of Counts. *arXiv preprint arXiv:2110.14790*.
- Kowal, D. R. and Canale, A. (2020). Simultaneous Transformation and Rounding (STAR) Models for Integer-Valued Data. *Electronic Journal of Statistics*, 14(1):1744–1772.
- Kowal, D. R. and Wu, B. (2021). Semiparametric count data regression for self-reported mental health. *arXiv preprint arXiv:2106.09114*.
- Liu, H., Lafferty, J., and Wasserman, L. (2009). The nonparanormal: Semiparametric estimation of high dimensional undirected graphs. *Journal of Machine Learning Research*, 10(10):2295–2328.
- Peluso, A., Vinciotti, V., and Yu, K. (2019). Discrete Weibull generalized additive model: an application to count fertility data. *Journal of the Royal Statistical Society: Series C (Applied Statistics)*, 68(3):565–583.

- Pitt, M., Chan, D., and Kohn, R. (2006). Efficient Bayesian inference for Gaussian copula regression models. *Biometrika*, 93(3):537–554.
- Polson, N. G., Scott, J. G., and Windle, J. (2013). Bayesian inference for logistic models using Pólya-Gamma latent variables. *Journal of the American Statistical Association*, 108(504):1339–1349.
- Scheipl, F., Fahrmeir, L., and Kneib, T. (2012). Spike-and-slab priors for function selection in structured additive regression models. *Journal of the American Statistical Association*, 107(500):1518–1532.
- Scott, J. G. and Berger, J. O. (2010). Bayes and empirical-Bayes multiplicity adjustment in the variable-selection problem. *The Annals of Statistics*, pages 2587–2619.
- Sellers, K. F. and Shmueli, G. (2010). A flexible regression model for count data. *The Annals of Applied Statistics*, pages 943–961.
- Siegfried, S. and Hothorn, T. (2020). Count transformation models. *Methods in Ecology and Evolution*, 11(7):818–827.
- Zellner, A. (1986). On assessing prior distributions and Bayesian regression analysis with g-prior distributions. *Bayesian inference and decision techniques*.

Supplementary materials

Supplementary materials include R code to reproduce the simulation studies from Section 3 and an R package available at www.GitHub.com/drkowal/rSTAR.

Appendix

Proof. (Theorem 2) Since Theorem 1 implies that $p(\theta | y)$ is a selection distribution under model (1)–(2), the joint Gaussian assumption in (8) implies that $p(\theta | y)$ is selection normal. The remaining properties follow from Arellano-Valle et al. (2006). \square

Proof. (Theorem 3) The result follows from the properties of the selection normal (Arellano-Valle et al., 2006) applied to model (1) and (8) via Theorem 2. \square

Proof. (Lemma 1) The result follows by direct computation as a consequence of Theorem 2 under the stated model (3) and prior $\theta \sim N(\mu_\theta, \Sigma_\theta)$. \square

Proof. (Lemma 2) Using Theorem 3, it is sufficient to compute Σ_z and $\Sigma_\theta - \Sigma'_{z\theta} \Sigma_z^{-1} \Sigma_{z\theta}$ under the linear model with the g-prior. By computing $\Sigma_z = \sigma^2 \{I_n + \psi X(X'X)^{-1} X'\}$ and applying the Woodbury identity, it follows that $\Sigma_z^{-1} = \sigma^{-2} \{I_n - \psi(1 + \psi)^{-1} X(X'X)^{-1} X'\}$, so $\Sigma'_{z\theta} \Sigma_z^{-1} = \psi(1 + \psi)^{-1} (X'X)^{-1} X'$ and $\Sigma'_{z\theta} \Sigma_z^{-1} \Sigma_{z\theta} = \sigma^2 \psi^2 (1 + \psi)^{-1} (X'X)^{-1}$. Observing that $\Sigma_\theta - \Sigma'_{z\theta} \Sigma_z^{-1} \Sigma_{z\theta} = \sigma^2 \psi (1 + \psi)^{-1} (X'X)^{-1}$ shows the result. \square

Proof. (Lemma 3) The selection normal prior is equivalently defined by $[\theta \mid z_0 \in \mathcal{C}_0]$ for $(z'_0, \theta')'$ jointly Gaussian with moments given in the prior. The posterior is constructed similarly: $[\theta \mid y] = [\theta \mid z_0 \in \mathcal{C}_0, z \in g(\mathcal{A}_y)] = [\theta \mid z \in \mathcal{C}_0 \times g(\mathcal{A}_y)]$ where $z_1 = (z'_0, z')'$. It remains to identify the moments of $(z'_1, \theta')' = (z'_0, z', \theta')'$. For each individual block of z_0, z , and θ and the pairs (z_0, θ) and (z, θ) , the moments are provided by the selection normal prior or the selection normal posterior in Lemma 1. All that remains is the cross-covariance $\text{Cov}(z_0, z) = \text{Cov}(z_0, X\theta + \epsilon) = \Sigma_{z_0\theta}X'$. \square

Proof. (Lemma 5) As a preliminary, consider a linear combination of a selection normal variable with a Gaussian innovation:

Lemma 9. *Suppose $\theta \sim \text{SLCT-}N_{n,p}(\mu_z, \mu_\theta, \Sigma_z, \Sigma_\theta, \Sigma_{z\theta}, \mathcal{C})$ and let $\theta^* = A\theta + a$ where A is a fixed $q \times p$ matrix and $a \sim N_q(\mu_a, \Sigma_a)$ is independent of θ . Then $\theta^* \sim \text{SLCT-}N_{n,q}(\mu_z, \mu_{\theta^*} = A\mu_\theta + \mu_a, \Sigma_z, \Sigma_{\theta^*} = A\Sigma_\theta A' + \Sigma_a, \Sigma_{z\theta^*} = \Sigma_{z\theta}A', \mathcal{C})$.*

Proof. (Lemma 9) First consider the distribution of $A\theta$. Since the moments of the joint distribution (z, θ) are given by assumption, it follows that $(z, A\theta)$ is jointly Gaussian and $[A\theta \mid z \in \mathcal{C}] \sim \text{SLCT-}N_{n,q}(\mu_z, A\mu_\theta, \Sigma_z, A\Sigma_\theta A', \Sigma_{z\theta}A', \mathcal{C})$. Using the moment generating functions and noting independence between $A\theta$ and a , it follows that $M_{\theta^*}(s) = M_{A\theta+a}(s) = M_{A\theta}(s)M_a(s)$ where $M_{A\theta}$ is in Theorem 2 and $M_a(s) = \exp(s'\mu_a + s'\Sigma_a s/2)$. The result of this product is the moment generating function of the stated selection normal distribution. \square

Returning to Lemma 5, the latent predictive variable $[\tilde{z} \mid \theta]$ in (13) can be represented as $\tilde{z} = \tilde{X}\theta + \tilde{\epsilon}$, where $\tilde{\epsilon} \sim N_n(0, \sigma^2 I_n)$ is independent of $\{\epsilon_i\}_{i=1}^n$ from (3). The integrand in (13) requires marginalization over $\theta \sim p(\theta \mid y)$, which is selection normal according to Lemma 1. Hence we obtain the latent predictive distribution $[\tilde{z} \mid y]$ via the marginalization from Lemma 9. \square

Proof. (Lemma 6) First, $\Sigma_z = \sigma^2\{I_n + \psi X(X'X)^{-1}X'\}$ is unchanged from Lemma 2. Similarly, using the generic notation from (8), we have $\Sigma'_{z\theta}\Sigma_z^{-1} = \psi(1 + \psi)^{-1}\tilde{X}(X'X)^{-1}X'$ and $\Sigma'_{z\theta}\Sigma_z^{-1}\Sigma_{z\theta} = \sigma^2\psi^2(1 + \psi)^{-1}\tilde{X}(X'X)^{-1}\tilde{X}'$. Computing $\Sigma_\theta - \Sigma'_{z\theta}\Sigma_z^{-1}\Sigma_{z\theta} = \sigma^2\{\psi(1 + \psi)^{-1}\tilde{X}(X'X)^{-1}\tilde{X}' + I_{\tilde{n}}\}$ shows the result for \tilde{z}^* . Since the link in (1) is deterministic, the result for \tilde{y}^* follows. \square

Proof. (Lemma 7) Computing the selection normal terms in the notation of (8), we have $\Sigma_z = \sigma^2(\psi XX' + I_n)$, $\Sigma_\theta = \sigma^2(\psi \tilde{X}\tilde{X}' + I_{\tilde{n}})$, and $\Sigma_{z\theta} = \psi\sigma^2 X\tilde{X}'$. Let $D_\psi = (\psi^{-1}I_p + X'X)^{-1} = \text{diag}\{\psi/(1 + \psi d_j)\}$, so $\Sigma_z^{-1} = \sigma^{-2}(I_n - XD_\psi X')$ by the Woodbury identity. Next, we derive $\Sigma'_{z\theta}\Sigma_z^{-1} = \psi\tilde{X}\{X' - (X'X)D_\psi X'\}$ and $\Sigma'_{z\theta}\Sigma_z^{-1}\Sigma_{z\theta} = \psi^2\sigma^2\tilde{X}\{(X'X) - (X'X)D_\psi(X'X)\}\tilde{X}'$, so $\Sigma_\theta - \Sigma'_{z\theta}\Sigma_z^{-1}\Sigma_{z\theta} = \psi\sigma^2\tilde{X}[I_p - \psi\{(X'X) - (X'X)D_\psi(X'X)\}]X' + \sigma^2 I_{\tilde{n}}$. Since $X'X = \text{diag}(d_j)$, the term in the square brackets is diagonal with elements $1 - \psi\{d_j - d_j^2\psi/(1 + \psi d_j)\} = 1/(1 + \psi d_j)$. Applying Lemma 6 shows the result. \square

Proof. (Lemma 8) The result follows from (15) applied to each model \mathcal{M}_k . \square